TECHNICAL NOTE

Interleaved water and fat MR thermometry for monitoring high intensity focused ultrasound ablation of bone lesions

Beatrice Lena[1] (iD) | **Lambertus W. Bartels**[1] | **Cyril J. Ferrer**[2] (iD) | **Chrit T. W. Moonen**[2] | **Max A. Viergever**[1] | **Clemens Bos**[2]

[1]Image Sciences Institute, University Medical Center Utrecht, Utrecht, the Netherlands

[2]Imaging Division, University Medical Center Utrecht, Utrecht, the Netherlands

Correspondence
Beatrice Lena, Image Sciences Institute, University Medical Center Utrecht, Utrecht, the Netherlands.
Email: b.lena@umcutrecht.nl

Funding information
PPP allowance of Top Sector Life Sciences & Health; Dutch Cancer Society; NWO Domain Applied and Engineering Sciences

Purpose: To demonstrate that interleaved MR thermometry can monitor temperature in water and fat with adequate temporal resolution. This is relevant for high intensity focused uUltrasounds (HIFU) treatment of bone lesions, which are often found near aqueous tissues, as muscle, or embedded in adipose tissues, as subcutaneous fat and bone marrow.

Methods: Proton resonance frequency shift (PRFS)-based thermometry scans and T_1-based 2D variable flip angle (2D-VFA) thermometry scans were acquired alternatingly over time. Temperature in water was monitored using PRFS thermometry, and in fat by 2D-VFA thermometry with slice profile effect correction. The feasibility of interleaved water/fat temperature monitoring was studied ex vivo in porcine bone during MR-HIFU sonication. Precision and stability of measurements in vivo were evaluated in a healthy volunteer under non-heating conditions.

Results: The method allowed observing temperature change over time in muscle and fat, including bone marrow, during MR-HIFU sonication, with a temporal resolution of 6.1 s. In vivo, the apparent temperature change was stable on the time scale of the experiment: In 7 min the systematic drift was <0.042°C/min in muscle (PRFS after drift correction) and <0.096°C/min in bone marrow (2D-VFA). The SD of the temperature change averaged over time was 0.98°C (PRFS) and 2.7°C (2D-VFA).

Conclusions: Interleaved MR thermometry allows temperature measurements in water and fat with a temporal resolution high enough for monitoring HIFU ablation. Specifically, combined fat and water thermometry provides uninterrupted information on temperature changes in tissue close to the bone cortex.

KEYWORDS
bone, high-intensity focused ultrasound, interleaved MRI, MR thermometry, PRFS, VFA

1 | INTRODUCTION

MRI-guided high intensity focused ultrasound (MR-HIFU) allows non-invasive treatments of various conditions[1] by thermal ablation, and its effectiveness for treatment of patients with painful bone metastases has been clinically demonstrated.[2] Pain reduction in these patients is achieved by ablation of the periosteum in the proximity of the metastases. MRI is a reliable guidance technique for HIFU, due to its excellent soft-tissue contrast and its capacity to map tissue temperature changes.[3] Temperature mapping is used to ensure that sufficient energy is delivered to reach an adequate thermal dose in the target zone, while preventing damage to surrounding healthy tissues.

In clinical procedures, proton resonance frequency shift (PRFS)-based thermometry has become the most used MR thermometry (MRT) technique for aqueous tissues.[5-7] Key factors are that the proton resonance frequency of hydrogen nuclei in water molecules varies linearly with temperature,[4] and is almost independent of tissue type. Moreover, PRFS thermometry has an easy implementation with rapid gradient echo (GRE) sequences.[8]

For the treatment of bone lesions, existing clinical protocols also rely on PRFS thermometry. Therefore, during treatments, temperature information is only available in voxels containing aqueous tissues, like muscle or tumor tissue.[7] Pure adipose tissues, as subcutaneous fat, and mixed adipose tissues, as bone marrow, are often found in and around bones. Thus, frequently, a mixture of fat- and water-based tissues is present in the target area. Moreover, the energy deposition within the ultrasound beam path can cause unwanted injuries in the area closest to the transducer.[9] Therefore, the heating should be monitored also in the subcutaneous fat.[10,11] For these reasons, temperature monitoring in both water and fat is desired for treatment of bone lesions.

The low water content and the absence of hydrogen bonding between fat molecules compromise the performance of PRFS thermometry in adipose tissues.[7] Alternative methods have been proposed to monitor temperature in fat, most of which have focused on T_1,[12,13] of which the temperature coefficient (in ms/°C) has been shown to be similar for the most prominent fat peak in different adipose tissues.[14]

To monitor temperature in an environment with both water and fat, Hey et al proposed a simultaneous PRFS/T_1 measurement technique using the variable flip angle (VFA) method. Aiming for real-time thermometry, they implemented the method using 2D GRE-echo planar imaging (EPI) sequences.[15] However, in 2D, the nonuniform flip angle (FA) profile in the slice direction causes errors in T_1 estimates and compromises the accuracy of T_1 mapping in fat.[16,17]

In more recent methods for simultaneous PRFS/2D-VFA thermometry,[18] a rescaling factor was applied to the FAs, to correct both for slice profile effects and for B_1 inhomogeneity. The rescaling factor was estimated experimentally for given T_1 values and was assumed to apply for all FAs between 5° and 90°. However, in these methods, PRFS thermometry was performed with short echo time (TE),[15,18] which limits the precision in PRFS temperature maps. Simultaneous measurements of PRFS and T_1 need to balance the precision of both measurements, leading to compromises for the echo time and the FA choice.

Here, we propose a 2D water-fat MR thermometry method based on an interleaved framework,[19] in which two sequences are independently optimized for the two tissue types: temperature in aqueous tissues is monitored using a PRFS sequence and in fat using 2D-VFA scans. The 2D-VFA settings are chosen to deliver accurate and precise T_1 estimates over a range of T_1, and T_1 maps are corrected for slice profile effects based on simulation that include the full slice profile.[20] The potential of this technique to provide temperature information in all soft tissues for monitoring MR-HIFU ablation of bone lesions was tested in ex vivo experiments. The stability of the method was investigated under in vivo conditions.

2 | METHODS

All experiments were performed with a clinical 1.5T MR scanner (Philips Achieva, Best, The Netherlands). Image processing was done offline using MatLab 2018a (Mathworks, Natick, MA).

2.1 | Identification of water and fat voxels

Prior to temperature mapping, it is crucial to identify water and fat voxels, to select which of the two temperature readouts will be applied. A three-point Dixon image was acquired to provide water and fat images.[21,22] Voxelwise, fat signal fraction maps were estimated using $S_{fat}\% = \frac{S_{fat}}{S_{InPhase}} \times 100$, where $S_{InPhase}$ and S_{fat} are the signal intensities in the reconstructed in-phase and fat image, respectively. An empirically chosen threshold, $S_{fat}\% = 70\%$ was then used to select the voxels in adipose tissues, that is, subcutaneous fat and bone marrow, as identified on anatomical images.

2.2 | Calculation of temperature maps

A framework allowing fast switching between pulse sequences[19] was used to interleave acquisition of one PRFS scan with one 2D-VFA T_1 scan, which consists of two T_1-weighted (T1w) images at different FAs (Figure 1). For temperature monitoring, we acquired a set of five reference
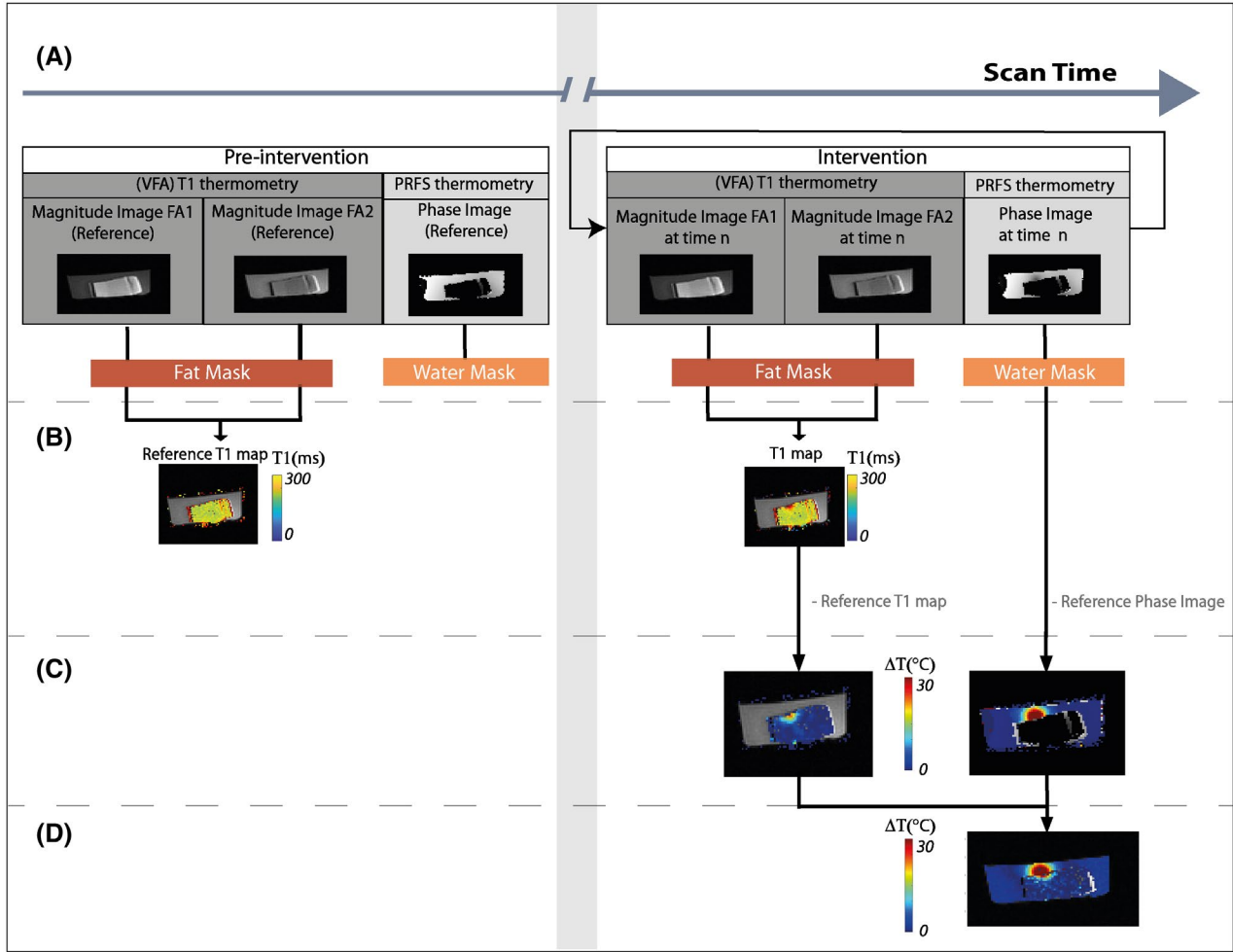
FIGURE 1 A, Fat and water images acquired with the interleaved framework (magnitude images at two FAs for 2D-VFA MRT and phase images for PRFS MRT). B, 2D-VFA T_1 mapping. C, 2D-VFA-based and PRFS-based MRT calculation. D, Fusion of MRT images

PRFS phase maps and five reference VFA T_1 maps before heating and continued acquiring interleaved PRFS and 2D-VFA images during the heating and cool-down phases (Figure 1A).

2.2.1 | VFA-based fat MR thermometry

T_1 maps for fat thermometry were obtained via the linearized form of the steady-state signal equation:

$$\frac{S}{\sin\theta} = E_1 \frac{S}{\tan\theta} + M_0 (1 - E_1) \tag{1}$$

where S is the magnitude signal of a spoiled GRE image, $E_1 = e^{-\frac{TR}{T_1}}$, M_0 is the equilibrium magnetization, and θ is the FA. After acquiring the signal at two FAs, T_1 was estimated from Equation (2) by determining the slope of $S/\sin\theta$ vs $S/\tan\theta$.[23]

Since the method was applied in 2D, a correction for the slice profile effect was applied.[24,25] We corrected the VFA

T_1 maps by means of a T_1 look-up table (LUT), obtained by Bloch simulations including slice profile effects. Briefly, for an input T1 value and two FAs, the steady state signals were calculated and used to find the apparent longitudinal relaxation time using the conventional VFA T_1 estimation. The apparent T_1 includes the effects of the non-uniform slice excitation. Finally, by repeating the simulation for a range of T_1 values, and FAs, an LUT was created from which a slice-profile corrected T_1 can be retrieved based on the apparent T_1. In this procedure, B_1 inhomogeneity is compensated for by scaling the FAs. A T_1 LUT with scan parameters as applied in the experiment was generated once prior to the MRT experiment.

The temperature change (ΔT) maps, defined as the difference between the temperature at a time point t_n and the initial temperature, are inferred from the T_1 maps (Figure 1B), according to:

$$\Delta T_{fat}(t_n) = \sum_{i=1}^{n} \left(\frac{B}{\ln \frac{A}{T_1(t_i)}} - \frac{B}{\ln \frac{A}{T_1(t_{i-1})}} \right) \tag{2}$$

where $T_1(t_i)$ is the T_1 at a time point t_i and $T_1(t_{1-i})$ is the T_1 at a previous time point t_{i-1}. A (ms) and B (°C) are fit parameters from the exponential relation describing the dependence of T_1 on temperature, with $A = 2.59 \times 10^5$ ms and $B = 2.09 \times 10^3$ °C as determined for breast adipose tissues at 1.5T by Baron et al.[13]

2.2.2 | PRFS-based water MRT

Temperature change (ΔT) maps in water were determined from the phase images of a spoiled GRE scan with EPI. The temperature change is obtained by subtracting the reference phase $\varphi(t_0)$, at $t = t_0$ before the onset of temperature change, from the current phase at time t, $\varphi(t)$, during heating:

$$\Delta T_{water}(t) = \frac{\varphi(t) - \varphi(t_0)}{\gamma \alpha T E B_0} \quad (3)$$

where γ is the gyromagnetic ratio, α is the temperature coefficient of the shielding constant (0.010 ppm/°C), B_0 is the magnetic field strength, and TE is the echo time (Figure 1C). A correction for phase drift was applied[3,7]: drift was estimated from the average phase value in an unheated region from the PRFS scans. From this value, the temperature drift ΔT_{drift} was estimated using Equation (3) and subtracted to correct the temperature change maps.

2.3 | Ex vivo MR-HIFU heating experiment

Interleaved MRT was tested in an ex vivo experiment using HIFU heating. Experiments were performed on a clinical HIFU platform (Sonalleve MR-HIFU V2; Profound Medical,

Mississauga, Ontario, Canada). Images were acquired using the integrated two-element coil inside the tabletop of the HIFU system and a 16-element flat array coil.

The phantom consisted of a water tank, in which an excised lower hind leg of a pig was immersed (Figure 2) in degassed water. The intrinsic focus of the ultrasound transducer is an ellipsoid with dimensions of $2 \times 2 \times 7$ mm³, defined by the −3 dB level, where the longest dimension is along the ultrasound beam direction. MR thermometry was performed during 7 min. The heating experiment consisted of 50 s before heating, 60 s of HIFU sonication at 1.2 MHz with a constant acoustic power of 40 W and a cool-down period of 350 s.

A transverse temperature mapping slice was positioned through the focus. For PRFS-MRT, sequence parameter settings included binomial water selective excitation, TE = 19 ms, TR = 37 ms, FA = 20°, EPI factor = 11, phase encoding bandwidth 40 Hz/pixel. For VFA-MRT, TE = 4.6 ms, TR = 10 ms, FA = 6°-40°, readout bandwidth 136 Hz/pixel. For both sequences, 200×200 mm² FOV was used, with an acquired voxel size of $2 \times 2 \times 7$ mm³; number of dummy excitations for dynamics = 150, RF spoiling phase increment = 117°. Temperature maps were generated 6.1 s apart, that is, the duration of a cycle of two 2D-VFA scans and one PRFS scan. In-plane B1 inhomogeneities were corrected using B1 maps, acquired using the actual FA imaging method[26]: TR_1 30 ms, TR_2 150 ms, TE 4.40 ms, FA 60°.

2.4 | Non-heating demonstration on a volunteer

An in vivo demonstration was performed in one healthy volunteer without heating, with the approval of the
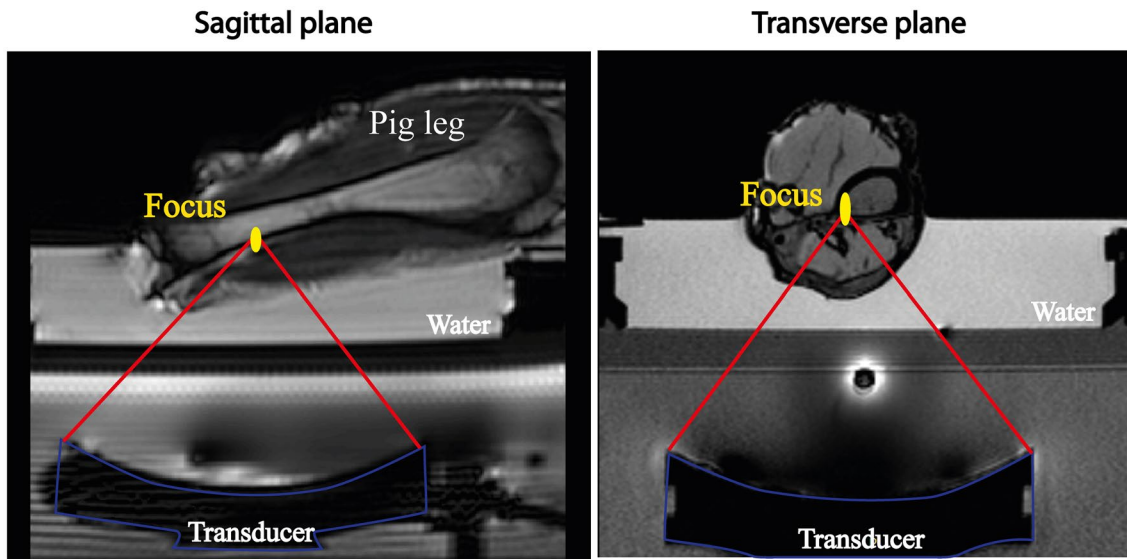

FIGURE 2 Experimental setup for the ex vivo experiment. The ultrasound transducer is outlined in blue and the ultrasound beam path in red. The imaging slice was positioned to match the focal location (in yellow)

institutional review board of the University Medical Center Utrecht (NL53099.041.15), and written informed consent was obtained from the volunteer. A transverse MRT slice was positioned in the lower leg of the volunteer. The same sequences and parameter settings as in the phantom experiment were used. A 16-element receive coil was used for signal reception.

Water and fat regions were set using three-point Dixon images,[21,22] as before. Using the method described above, 2D-VFA-based temperature maps were calculated in fat. To assess precision, a map of the temporal ΔT_{fat} SD was generated.

Finally, the capability of the proposed method to spatially resolve temperature changes (ie, as a temperature mapping technique) was evaluated. To this end, we first applied a rotationally symmetric Gaussian filter[30] with SD of one pixel for spatial low-pass filtering of the calculated temperature change maps. The range and the drift of the apparent temperature variations were characterized with their 10th (P10) and 90th (P90) percentile values and the slope of the linear regression of the estimates over the 7 min scan duration. P10, P90, and the slope of the linear fit were evaluated in 3 voxels each, in the muscle and the bone marrow.

3 | RESULTS

3.1 | Ex vivo MR-HIFU heating experiment

Using 2D-VFA-MRT, it was possible to detect the temperature changes in fat caused by HIFU heating. The temperature evolution was followed in three locations (Figure 3A): two voxels in the bone marrow at different distances from the focal point and one voxel in an adipose tissue layer near the focal point (Figure 3B). A temperature rise of 20°C was

seen in the bone marrow behind the cortex. The three curves show that the voxel closest to the focal point has the largest temperature change, whereas in the other locations, a lower temperature change is detected.

Close to the focal point, two voxels in muscle and bone marrow show a temperature peak ~120 s after the beginning of the experiment (Figure 3C). In the cool-down phase, the behavior of these voxels differs substantially: the temperature in fat decreases rapidly and returns to baseline, whereas the muscle maintains an elevated temperature after the sonication ended.

The combined water-fat temperature change map at 120 s, Figure 4C, shows a heated region that is continuous across the water-fat boundaries. A temperature rise of over 20°C was detected in the focal point area. Between 6 mm and 10 mm from the focal point, the detected temperature increase was still over 10°C. These observations are consistent with heat transfer from a region of intense heating at the bone cortex, which served as a heat source for surrounding tissues. However, in the cortical bone no temperature information was available, owing to a lack of MR signal.

Videos showing the whole MR-HIFU experiment are provided as Supporting Information Video S1, which is available online).

3.2 | Non-heating demonstration on a volunteer

The temporal SD map of ΔT_{fat} in fat voxels of a volunteer leg shows that $\sigma(\Delta T_{fat}) < 1°C$ in the subcutaneous fat and 2-3°C in the bone marrow (Figure 5A). We observed that $\sigma(\Delta T_{fat})$ is high where SNR is low, probably due to differences in coil sensitivity. Moreover, $\sigma(\Delta T_{fat})$ increased up to
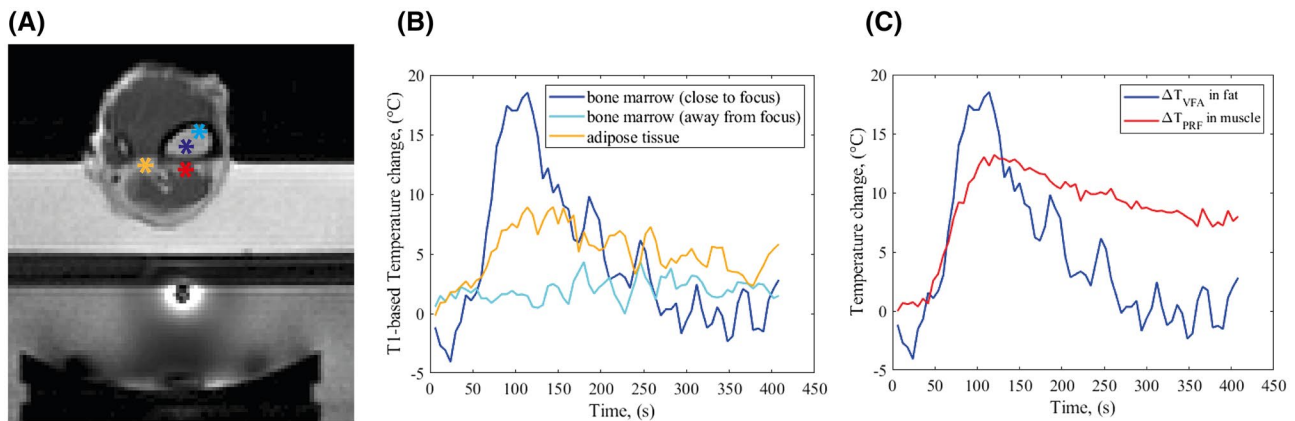

(A) **(B)** **(C)**

FIGURE 3 Combined water and fat thermometry during a HIFU sonication experiment. A, the asterisks indicate the location of the voxels considered. B, 2D-VFA-based temperature changes (°C) vs time estimated in fat voxels. C, Temperature changes vs time estimated using 2D-VFA-based MRT in fat and using PRFS-based MRT in muscle
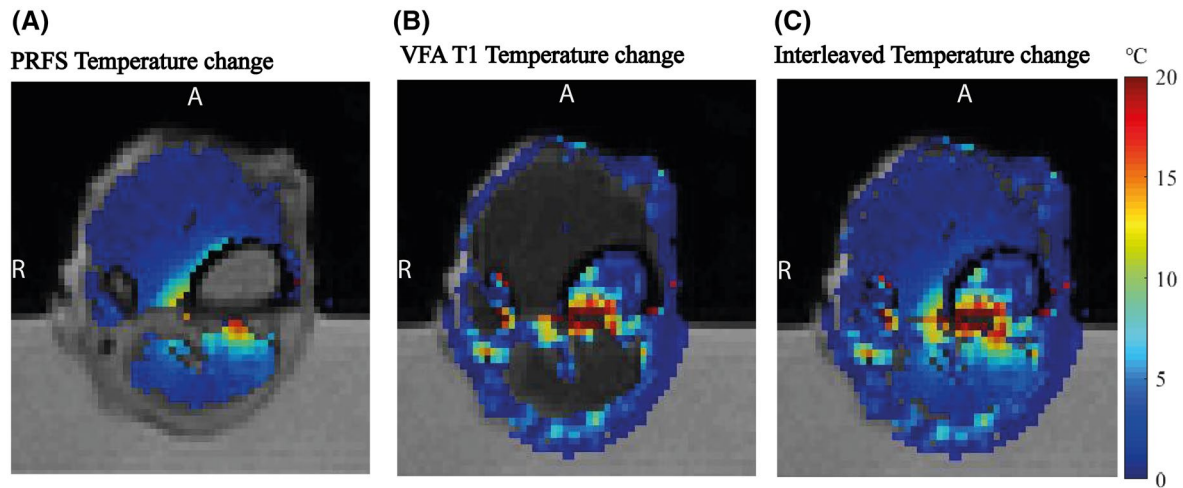
(A) PRFS Temperature change

(B) VFA T1 Temperature change

(C) Interleaved Temperature change

FIGURE 4 Temperature change maps at the temperature peak. A, From PRFS in water voxels. B, From 2D-VFA T1 in fat voxels. C, Overlaying the two maps, a temperature change map from the interleaved thermometry is provided

8°C at the fat-muscle interfaces, probably caused by partial volume effects.

Since the method is envisioned to be used as a mapping technique, the stability of temperature changes was estimated for individual locations (Figure 5B). For all the estimates, the temperature drift was below 0.5°C/min. The spread of the apparent temperature variations at the individual timepoints was further characterized by P10 and P90. For 2D-VFA-MRT, P10 was found between −2.5°C and −3.7°C, P90 between 1.5°C and 2.7°C. For PRFS-MRT, P10 was found between −0.74°C and −0.35°C, P90 between 0.18°C and 0.91°C.

4 | DISCUSSION

In this study, we have demonstrated the use of an interleaved scanning approach that enables monitoring temperature changes both in aqueous tissues (with PRFS-MRT) and in adipose tissues (with 2D-VFA-MRT). This method could aid monitoring HIFU treatments of bone metastases, for which both adipose and aqueous tissues can be found in the vicinity of the target. The feasibility of this approach was investigated in an MR-HIFU sonication experiment on an ex vivo porcine bone phantom. The method was shown to provide temperature measurements in nearly all tissues in the slice, both fatty tissues, and in any voxels containing sufficient water signal. Finally, the method was shown to be precise and stable enough for being used as a mapping technique in an in vivo experiment, with a temperature SD below 3°C in the bone marrow and negligible systemic temperature drift identified over the scan duration.

With interleaved MRT, it becomes possible to monitor complex heating behavior. In our experiment, this approach allowed to detect temperature change caused by transfer of

heat generated by the intersection of the ultrasound beam with the cortex[27] into the tissues surrounding the focal area.

MRT is generally used to measure temperature change rather than absolute temperature. Therefore, for the utility of the method, precision and stability over time change here are key parameters. Based on the precision measurements in bone marrow in vivo, we expect that temperature rises of the order of 3°C can be detected. Moreover, the temperature estimates in our experiments were computed continuously for 7 min, which resembles the time window of the HIFU sonication protocol (pre-scanning, sonication,[28] cool-down[10]) in clinical care. During this time, the 90th percentile of apparent temperature change observed in the single voxels in bone marrow was 1.5-2.7°C, which was likely caused by noise in the 2D-VFA source images. For HIFU ablation, the aim is to achieve temperatures above 60°C in the target area (ie, temperature changes of more than 23°).[29] Therefore, with the precision and the stability observed in our experiment, we expect that this method could improve the monitoring of temperature changes caused by HIFU ablation in the anatomy imaged.

Adding fat temperature information is relevant for treatment of bone metastases and tumors, where both the target and the surrounding area can contain adipose tissues.[30] Temperature mapping in water *and* fat may improve monitoring of heating also during other clinical applications of HIFU in target areas containing aqueous and adipose tissues, such as breast[13] and pancreas.[31]

While this study has demonstrated the temperature monitoring ability of the proposed technique, there are several limitations that must be addressed before this sequence may be offered for clinical use.

First, the image processing and temperature estimations were performed offline; therefore, the potential of interleaved MRT to perform real-time treatment monitoring has not been
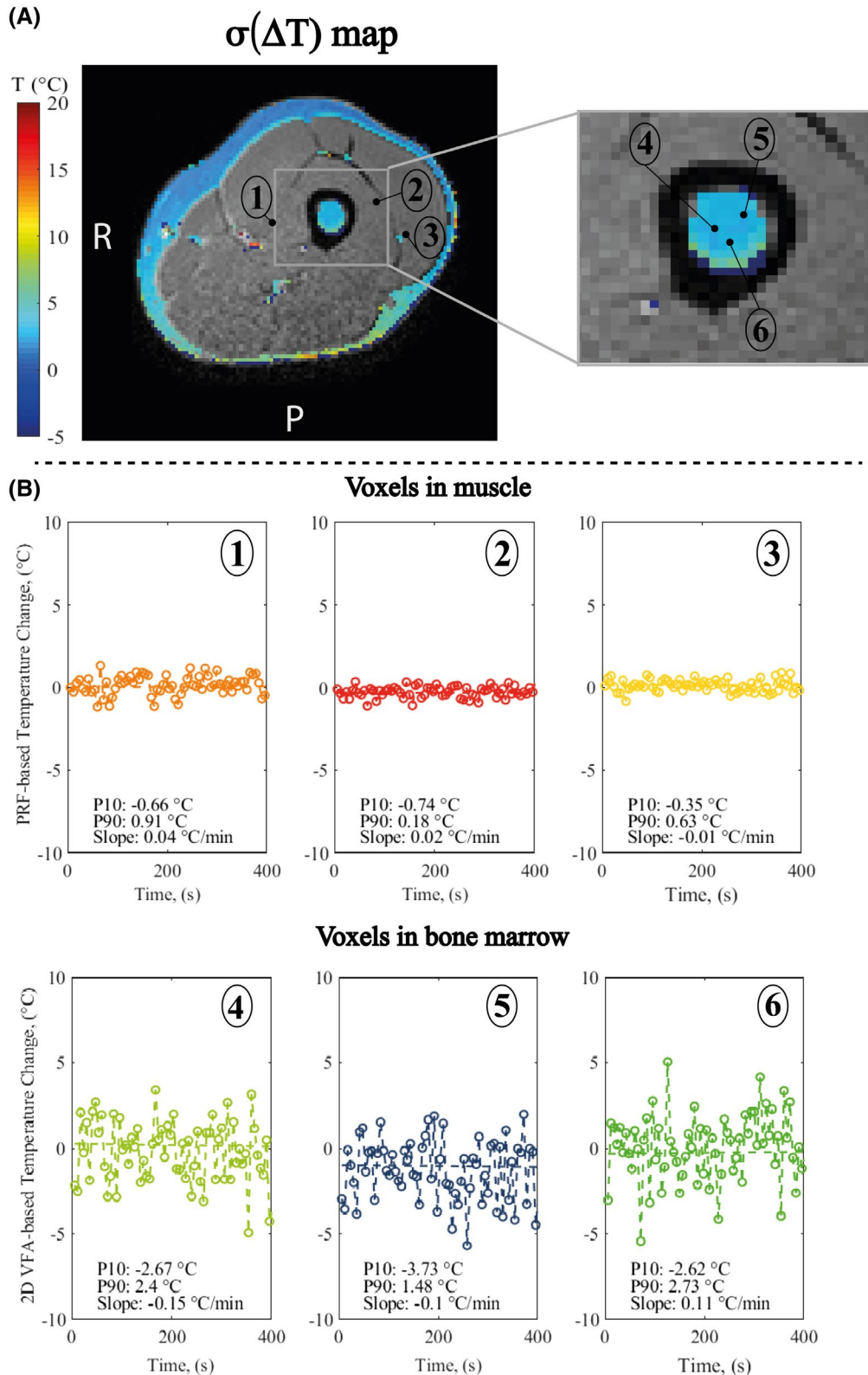
FIGURE 5 A, Temporal SD map of VFA-based temperature change in fat voxels of a transverse slice, located on the lower leg of a volunteer. B, Temperature change estimates, after spatial averaging with a gaussian filter, in the volunteer study without heating: 2D-VFA-based temperature changes in three voxels in the bone marrow and PRFS-based temperature change in three voxels in the muscle

tested yet. To apply interleaved MRT, water and fat masks were used. However, in case of motion during the scan session, a mismatch of fat and water voxels can occur between the mask (created prior to MRT) and the images from MRT scans. For our use case, that is, MRT for HIFU therapy of bones, this is less problematic as patients are usually sedated

but for other applications this mismatch could be mitigated by registration techniques or dynamic updates of the mask image, for example, using a multi-echo MRT pulse sequence, as was used by Poorman et al.[32]

The selection of the water and fat regions is key in view of the poor results of T_1 thermometry in voxels with mixed water and fat contributions. Here, a visualization approach based on masks was adopted to avoid partial volume effects. However, the problem could also be solved in acquisition, with fat/water suppression and water–fat separation methods.[33]

Moreover, fat thermometry relies on the VFA approach, which is known to be susceptible to B_1 inhomogeneties.[34] In this work, we acquired a B_1 map to correct for B_1 inhomogeneities. However, in case of more homogeneous B_1 fields, B_1 corrections might be omitted to save time.

Finally, the 6 s overall acquisition time of the technique described here imposes a minimum duration on the heating time, to enable temperature monitoring. In particular the time required to reach the steady state adds to the scan time for the VFA method. This issue has been addressed by Svedin et al,[35] who proposed to only acquire dynamic images at one FA during the MRT experiment, thus improving the VFA temporal resolution.

5 | CONCLUSIONS

In conclusion, interleaved PRFS and 2D-VFA T_1 thermometry enables temperature monitoring in fat and water for MR-HIFU treatments, showing the heat distribution inside and outside the bone across tissues of different composition. As such, the method holds potential for monitoring MR-HIFU in patients with bone lesions, thus contributing to the safety of treatments.

ORCID
Beatrice Lena https://orcid.org/0000-0001-9283-5918
Cyril J. Ferrer https://orcid.org/0000-0001-9804-5626

REFERENCES
1. Siedek F, Yeo SY, Heijman E, et al. Magnetic resonance-guided high-intensity focused ultrasound (MR-HIFU): technical background and overview of current clinical applications (Part 1). *RoFo Fortschritte auf dem Gebiet der Rontgenstrahlen und der Bildgebenden Verfahren.* 2019;191:522-530.

2. Scipione R, Anzidei M, Bazzocchi A, et al. HIFU for bone metastases and other musculoskeletal applications. *Semin Intervent Radiol.* 2018;35:261-267.

3. Rieke V, Pauly KB. MR thermometry. *J Magn Reson Imaging.* 2008;27:376-390.

4. Kuroda K. Non-invasive MR thermography using the water proton chemical shift. *Int J Hyperth.* 2005;21:547-560.

5. de Senneville BD, Mougenot C, Quesson B, Dragonu I, Grenier N, Moonen CTW. MR thermometry for monitoring tumor ablation. *Eur Radiol.* 2007;17:2401-2410.

6. Winter L, Oberacker E, Paul K, et al. Magnetic resonance thermometry: methodology, pitfalls and practical solutions. *Int J Hyperth.* 2016;32:63-75.

7. Odéen H, Parker DL. Magnetic resonance thermometry and its biological applications—physical principles and practical considerations. *Prog Nucl Magn Reson Spectrosc.* 2019;110:34-61.

8. Stollberger R, Ascher PW, Huber D, et al. Temperature monitoring of interstitial thermal tissue coagulation using MR phase images. *J Magn Reson Imaging.* 1998;8:188-196.

9. Mougenot C, Köhler MO, Enholm J, Quesson B, Moonen C. Quantification of near-field heating during volumetric MR-HIFU ablation. *Med Phys.* 2011;38:272-282.

10. Baron P, Ries M, Deckers R, et al. In vivo T2-based MR thermometry in adipose tissue layers for high-intensity focused ultrasound near-field monitoring. *Magn Reson Med.* 2014;72:1057-1064.

11. Lam MK, de Greef M, Bouwman JG, et al. Multi-gradient echo MR thermometry for monitoring of the near-field area during MR-guided high intensity focused ultrasound heating. *Phys Med Biol.* 2015;60:7729-7746.

12. Parker DL. Applications of NMR imaging in hyperthermia: an evaluation of the potential for localized tissue heating and noninvasive temperature monitoring. *IEEE Trans Biomed Eng.* 1984;BME-31:161-167. https://doi.org/10.1109/TBME.1984.325382

13. Baron P, Deckers R, Knuttel FM, Bartels LW. T1 and T2 temperature dependence of female human breast adipose tissue at 1.5 T: groundwork for monitoring thermal therapies in the breast. *NMR Biomed.* 2015;28:1463-1470.

14. Kuroda K, Iwabuchi T, Obara M, et al. Temperature dependence of relaxation times in proton components of fatty acids. *Magn Reson Med Sci.* 2011;10:177-183.

15. Hey S, de Smet M, Stehning C, et al. Simultaneous T1 measurements and proton resonance frequency shift based thermometry using variable flip angles. *Magn Reson Med.* 2012;67:457-463.

16. Svedin BT, Parker DL. Technical note: The effect of 2D excitation profile on T1 measurement accuracy using the variable flip angle method with an average flip angle assumption. *Med Phys.* 2017;44:5930-5937.

17. Parker GJM, Barker GJ, Tofts PS. Accurate multislice gradient echo T1 measurement in the presence of non-ideal RF pulse shape and RF field nonuniformity. *Magn Reson Med.* 2001;45:838-845.

18. Todd N, Diakite M, Payne A, Parker DL. Hybrid proton resonance frequency/T1 technique for simultaneous temperature monitoring in adipose and aqueous tissues. *Magn Reson Med.* 2013;69:62-70.

19. Henningsson M, Mens G, Koken P, Smink J, Botnar RM. A new framework for interleaved scanning in cardiovascular MR: application to image-based respiratory motion correction in coronary MR angiography. *Magn Reson Med.* 2015;73:692-696.

20. Braskute I, Deckers R, Viergever MA, Moonen CTW, Bartels LW. Bloch simulation-based correction for 2D VFA T1 mapping for fat MR thermometry. In Proceedings: Joint Annual Meeting ISMRM-ESMRMB; 2018; Paris, France. Abstract #4038.

21. Glover GH, Schneider E. Three-point dixon technique for true water/fat decomposition with B0 inhomogeneity correction. *Magn Reson Med*. 1991;18:371-383.

22. Lefebvre G. One sequence, many benefits in musculoskeletal MRI. *Fieldstrength*. 2015;18-21. Special issue ISMRM 2015.

23. Deoni SCL, Rutt BK, Peters TM. Rapid combined T1 and T2 mapping using gradient recalled acquisition in the steady state. *Magn Reson Med*. 2003;49:515-526.

24. Lena B, Bos C, Moonen CTW, Viergever MA, Bartels LW. Flip angle optimization and in vitro demonstration of 2D DESPOT1-based fat thermometry. In Proceedings: ISMRM 27th Annual Meeting & Exhibition; 2019; Montréal, QC, Canada. Abstract #3829.

25. Lena B, Bos C, Ferrer CJ, Moonen CTW, Viergever MA, Bartels LW. Rapid 2D variable flip angle method for accurate and precise T1 measurements over a wide range of T1 values. *NMR Biomed*. 2021. http://dx.doi.org/10.1002/nbm.4542.

26. Yarnykh VL. Actual flip-angle imaging in the pulsed steady state: a method for rapid three-dimensional mapping of the transmitted radiofrequency field. *Magn Reson Med*. 2007;200:192-200.

27. Bitton RR, Webb TD, Pauly KB, Ghanouni P. Prolonged heating in nontargeted tissue during MR-guided focused ultrasound of bone tumors. *J Magn Reson Imaging*. 2019;50:1526-1533.

28. Huisman M, Lam MK, Bartels LW, et al. Feasibility of volumetric MRI-guided high intensity focused ultrasound (MR-HIFU) for painful bone metastases. *J Ther Ultrasound*. 2014;2:1-10.

29. Fu F, Xin SX, Chen W. Temperature-and frequency-dependent dielectric properties of biological tissues within the temperature and frequency ranges typically used for magnetic resonance imaging-guided focused ultrasound surgery. *Int J Hyperth*. 2014;30:56-65.

30. Kremer R, Gilsanz V. Fat and bone: an odd couple. *Front Endocrinol*. 2016.6 1–12.

31. Wu F. High intensity focused ultrasound: a noninvasive therapy for locally advanced pancreatic cancer. *World J Gastroenterol*. 2014;20:16480-16488.

32. Poorman ME, Braškutė I, Bartels LW, Grissom WA. Multi-echo MR thermometry using iterative separation of baseline water and fat images. *Magn Reson Med*. 2019;81:2385-2398.

33. Bley TA, Wieben O, François CJ, Brittain JH, Reeder SB. Fat and water magnetic resonance imaging. *J Magn Reson Imaging*. 2010;31:4-18.

34. Sung K, Daniel BL, Hargreaves BA. Transmit B1+ field inhomogeneity and T1 estimation errors in breast DCE-MRI at 3 Tesla. *J Magn Reson Imaging*. 2013;38:454-459.

35. Svedin BT, Payne A, Parker DL. Simultaneous proton resonance frequency shift thermometry and T1 measurements using a single reference variable flip angle T1 method. *Magn Reson Med*. 2019;81:3138-3152.

SUPPORTING INFORMATION

Additional Supporting Information may be found online in the Supporting Information section.

VIDEOS S1 Combined water and fat thermometry during the whole HIFU sonication experiment. Temperature change maps from PRFS in water voxels (A) and from 2D-VFA T1 in fat voxels (B). Overlaying the two maps, a temperature change map from the interleaved thermometry is provided (C)